The *closo*-$\mathrm{Pb_{10}}^{2-}$ Zintl ion in the $[\mathrm{Ni@Pb_{10}}]^{2-}$ cluster

Emren N. Esenturk, James Fettinger and Bryan Eichhorn*

Received (in Cambridge, UK) 5th August 2004, Accepted 21st September 2004
First published as an Advance Article on the web 25th October 2004
DOI: 10.1039/b412082e

The cluster $[\mathrm{Ni@Pb_{10}}]^{2-}$, prepared from $\mathrm{Pb_9}^{4-}$ and $\mathrm{Ni(COD)_2}$, contains a new Zintl ion subunit, closo-$\mathrm{Pb_{10}}^{2-}$, centered by a Ni atom.

The group 14 polyatomic anions are prominent members of the Zintl ion family. Their chemistry is dominated by nine-atom clusters with boron-hydride-like structures. Examples include the naked $\mathrm{E_9}^{x-}$ ions where E = Si–Pb, x = 3,4 (see I, II),[1] the $[(\mathrm{Ge_9})_2]^{6-}$ dimer, $[(\mathrm{Ge_9})_3]^{6-}$ trimer, $[(\mathrm{Ge_9})_4]^{8-}$ tetramer, and ${}^{1}_{\infty}[\mathrm{Ge_9}^{2-}]$ polymer formed by oxidative coupling of *nido*-$\mathrm{Ge_9}^{4-}$ clusters.[2–4] These anions have been studied extensively due to their simplicity, high reactivity and their potential utility in the preparation of nanomaterials.[1] The *closo*-$[\mathrm{Sn_9M(CO)_3}]^{4-}$ complexes where M = Cr, Mo, W (see III)[5] are transition metal derivatives of the *nido*-$\mathrm{Sn_9}^{4-}$ ion with virtually unperturbed $\mathrm{Sn_9}^{4-}$ subunits capped by $\mathrm{M(CO)_3}$ fragments. However, most transition metal derivatives of the $\mathrm{E_9}^{4-}$ ions contain main group fragments with different structures and/or nuclearities. Structurally modified 9-atom clusters include the tricapped trigonal prismatic $\mathrm{Sn_9}$ cluster in the $[\mathrm{Sn_9Pt_2(PPh_3)}]^{2-}$ complex[6] and the open $\mathrm{Sn_9}$ framework in the *closo*-$[\eta^5\text{-}\mathrm{Sn_9W(CO)_3}]^{4-}$ isomer.[5] New Zintl ions are also stabilized by transition metal fragments as exemplified by the complexes *closo*-$[\mathrm{Sn_6\{Cr(CO)_5\}_6}]^{2-}$, $\{\mathrm{Sn_6[Nb(tol)]_2}\}^{2-}$ and $[\mathrm{Pt@Pb_{12}}]^{2-}$ that contain the previously unknown $\mathrm{Sn_6}^{2-}$, $\mathrm{Sn_6}^{12-}$ and $\mathrm{Pb_{12}}^{2-}$ ions, respectively.[7–9] The latter complex represents a rare example of an endohedral naked metal cluster and, due to their high symmetry and potential σ-aromaticity, this class of clusters has received much attention of late.[10–14] Extensive theoretical studies[15–19] have been performed on hypothetical members of this class, but only a few gas phase studies[20–22] suggest their existence and structural data are sparse. Here, we report the synthesis, structure and properties of a new member of this class of endohedral clusters, $[\mathrm{Ni@Pb_{10}}]^{2-}$, which contains a Ni atom centered in a *closo*-$\mathrm{Pb_{10}}^{2-}$ bicapped square antiprism. The *closo*-$\mathrm{Pb_{10}}^{2-}$ cluster is a new type of Zintl ion.

Solutions of $\mathrm{K_4Pb_9}$ in ethylenediamine (en) react with solutions of $\mathrm{Ni(COD)_2}$ in toluene (tol) in the presence of 2,2,2-crypt to give moderate yields of the $[\mathrm{Ni@Pb_{10}}]^{2-}$ ion as the $[\mathrm{K(2,2,2\text{-}crypt)}]^{+}$ salt. The crystalline solid is dark brown and forms stable reddish brown solutions in dimethylformamide (dmf) and dimethyl sulfoxide (dmso). The compound is air and moisture sensitive in solution and the solid state. Small quantities ($<\sim 10\%$) of $[\mathrm{K(2,2,2\text{-}crypt)}]_2[\mathrm{Ni@Pb_{12}}]$ co-crystallize with the title complex.† $[\mathrm{Ni@Pb_{12}}]^{2-}$ is isostructural with the $[\mathrm{Pt@Pb_{12}}]^{2-}$ anion[9] and will be described in a subsequent publication. The salt has been characterized by single crystal XRD, energy-dispersive X-ray analysis (EDX), ^{207}Pb NMR and laser desorption/ionization-time of-flight mass spectrometry (LDI-TOF MS).

The $[\mathrm{Ni@Pb_{10}}]^{2-}$ anion crystallizes with two $[\mathrm{K(2,2,2\text{-}crypt)}]^{+}$ cations in the monoclinic system, space group *C*2/*c*.‡ The anion possesses virtual D_{4d} point symmetry and is defined by a 10-vertex $\mathrm{Pb_{10}}^{2-}$ bicapped square antiprism centered by a Ni atom (Fig. 1). According to the conventions for Wade's rules of electron counting,[23] the Pb and Ni atoms donate two electrons and zero electrons to cluster bonding, respectively, that result in a 22 electron, $2n$+2 framework with a *closo* geometry when the −2 charge of the cluster is taken into consideration. The two axial Pb–Ni contacts are elongated (3.210(3) Å (av)) in comparison with the other eight Pb–Ni bonds in the complex (2.722(2) Å (av)). The 24 Pb–Pb contacts of the $\mathrm{Pb_{10}}$ deltahedron can be categorized into three different types. The average distances to the capping Pb atom (Pb1) are the shortest at 3.094(2) Å. The Pb–Pb contacts between square planes are intermediate at 3.135(3) Å (av) whereas the distances between Pb atoms within the square planes are the longest at 3.405(2) Å (av). A recent theoretical study by Schrodt *et al.* of stable binary metal atom clusters suggested that the neutral bicapped square antiprism, $\mathrm{Pb_{10}Ni}$, with D_{4d} point symmetry is the most stable isomer.[24] Their DFT calculations predicted Pb–Pb bond distances of 3.12–3.21 Å and Pb–Ni distances of 2.89–2.99 Å, which are reasonably close to the

I

II

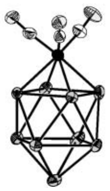

III

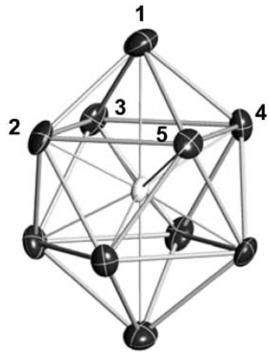

Fig. 1 ORTEP drawing of the $[\mathrm{Ni@Pb_{10}}]^{2-}$ ion showing bicapped square antiprism structure. Ni is gray, Pb is black, thermal ellipsoids are set at the 50% probability level.

---

*eichhorn@umd.edu

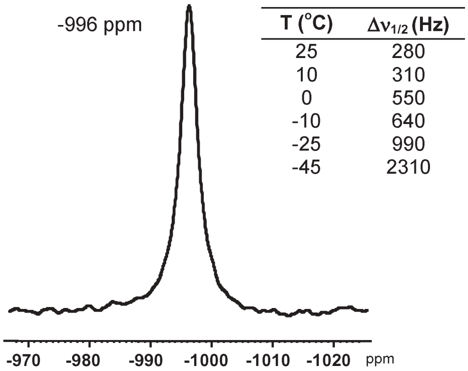

T (°C)	Δν$_{1/2}$ (Hz)
25	280
10	310
0	550
-10	640
-25	990
-45	2310

Fig. 2 ^{207}Pb NMR spectrum of the $[Ni@Pb_{10}]^{2-}$ ion recorded in dmf at 25 °C and 104.7 MHz. Table show change in line width ($\Delta\nu_{1/2}$) with temperature.

experimental results reported here. The discrepancies presumably result from the differences in charge between the model and the isolated cluster, which finds the latter in a more axially-elongated structure. A similar centered 10-atom cluster with a *closo* structure type, *closo*-$[Zn@In_{10}]$, has been observed as a component in the solid-state structure of $K_{10}In_{10}Ni$.[25]

Despite the two distinct chemical environments of the lead atoms in the title complex, its ^{207}Pb NMR spectrum (Fig. 2) shows a single, broad resonance at −996 ppm ($\Delta\nu_{1/2}$ = 280 Hz, at 25 °C) due to dynamic exchange.§ For comparison, Pb_9^{4-} shows a relatively sharp resonance ($\Delta\nu_{1/2}$ = 47 Hz, at 25 °C) under the same conditions (104.7 MHz) as a result of fast exchange on the NMR time scale. When the temperature is decreased gradually, the line width of the Pb_{10} signal increases to 2310 Hz at −45 °C, which we interpret as slowing intramolecular exchange on the NMR time scale. However, we have yet to observe the limiting spectrum with the expected two, mutually-coupled resonances.

The LDI-TOF mass spectrum (negative ion mode) of the $[Ni@Pb_{10}]^{2-}$ complex shows distinctive mass envelopes associated with the $[Ni@Pb_{10}K]^{1-}$ and $[Ni@Pb_{10}]^{1-}$ ions (Fig. 3). The observation of the oxidized parent ion and K$^+$ ion pairs are common to Zintl clusters.[6,26] Interesting fragmentation patterns are observed for this and related clusters and a detailed report of the LDI-TOF-MS results will be described in a subsequent publication.[27]

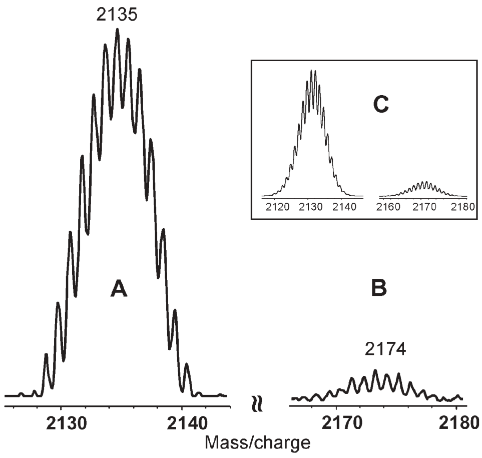

Fig. 3 LDI-TOF mass spectrum of the $[Ni@Pb_{10}]^{-1}$ (**A**) and $[Ni@Pb_{10}K]^{-1}$ (**B**) ions. The insets show the calculated mass envelope of the $[Ni@Pb_{10}]^{-1}$ and $[Ni@Pb_{10}K]^{-1}$ ions (**C**).

We thank the National Science Foundation for support of this work.

Emren N. Esenturk, James Fettinger and Bryan Eichhorn*
Department of Chemistry and Biochemistry University of Maryland,
College Park, Maryland 20742, USA. E-mail: eichhorn@umd.edu;
Fax: 301-314-9121

Notes and references

† *Preparation* of $[K(2,2,2\text{-crypt})]_2[Ni@Pb_{10}]$: In a drybox, K_4Pb_9 (80 mg, 0.04 mmol) and 2,2,2-crypt (59.6 mg, 0.158 mmol) were dissolved in en (~2 mL) in vial 1 yielding a dark green solution. In vial 2, $Ni(COD)_2$ (10.9 mg, 0.024 mmol) was dissolved in toluene (~1 mL) yielding a yellow solution. The solution from vial 2 was added drop wise to vial 1 and mixture was stirred ~2 h yielding a reddish brown solution. The solution was then filtered through tightly packed glass wool. Dark red crystals formed in the reaction vessel after 4–5 days (~25 mg, ~90 : 10 mixture of $[Ni@Pb_{10}]^{2-}$: $[Ni@Pb_{12}]^{2-}$ crystals). ^{207}Pb NMR (dmf, 25 °C): δ (ppm): −996 (*vs.* $Pb(NO_3)_2$(1M, D_2O, δ = −2961.2 ppm), $\nu_{1/2}$ = 280 Hz . LDI-TOF MS, *m*/*z* = 2174 $[Ni@Pb_{10}K]^{1-}$, 2135 $[Ni@Pb_{10}]^{1-}$.

‡ *X-Ray structure* for $[K(2,2,2\text{-crypt})]_2[Ni@Pb_{10}]$: A dark brown crystal 0.41 × 0.13 0.06 mm^3 was analyzed using a Bruker SMART1000 single crystal CCD-diffractometer operating at 173 K. Data were corrected for absorption (SADABS) and L-P effects and the structure solved and refined (against F^2) using the SHELXTL software package. The crystal was twinned and the data were deconvoluted using the Gemini and Saint Software packages. *Crystal Data*: Monoclinic, space group *C*2/*c*, a = 24.843(3) Å, b = 11.941(2) Å, c = 21.403(3) Å; V = 6302.7(14) Å^3, ρ_{calcd} = 3.121 g cm^{-3}, $3.78° < 2\theta < 50.00°$, Mo$_{K\alpha}$ radiation, $\mu(Mo_{K\alpha})$ = 27.074 mm^{-1}, 5758 unique reflns for 295 parameters. GOF (F^2) = 1.060, $R1$ = 0.0582, $wR2$ = 0.1645 for $I > 2\sigma(I)$ and $R1$ = 0.0827, $wR2$ = 0.1764 for all data. CCDC 245966. See http://www.rsc.org/suppdata/cc/b4/b412082e/ for crystallographic data in .cif or other electronic format.

§ *NMR data* were collected on a Bruker 400 Avance Spectrometer using 5 mm sample tubes and standard pluse sequences. Typically, 2000 transients were collected with 0.4 s delays.

1 T. F. Fassler, *Coord. Chem. Rev.*, 2001, **215**, 347.
2 L. Xu and S. C. Sevov, *J. Am. Chem. Soc.*, 1999, **121**, 9245.
3 (*a*) A. Ugrinov and S. C. Sevov, *J. Am. Chem. Soc.*, 2002, **124**, 10990; (*b*) A. Ugrinov and S. C. Sevov, *Inorg. Chem.*, 2003, **42**, 5789.
4 C. Downie, Z. J. Tang and A. M. Guloy, *Angew. Chem. Int. Ed.*, 2000, **39**, 338.
5 B. Kesanli, J. Fettinger and B. Eichhorn, *Chem. Eur. J.*, 2001, **7**, 5277.
6 B. Kesanli, J. Fettinger, D. R. Gardner and B. Eichhorn, *J. Am. Chem. Soc.*, 2002, **124**, 4779.
7 B. Schiemenz and G. Huttner, *Angew. Chem. Int. Ed.*, 1993, **32**, 297.
8 B. Kesanli, J. Fettinger and B. Eichhorn, *Angew. Chem. Int. Ed.*, 2001, **40**, 2300.
9 E. N. Esenturk, J. Fettinger, Y. F. Lam and B. Eichhorn, *Angew. Chem. Int. Ed.*, 2004, **43**, 2132.
10 M. Ohara, K. Koyasu, A. Nakajima and K. Kaya, *Chem. Phys. Lett.*, 2003, **371**, 490.
11 M. Menon, A. N. Andriotis and G. Froudakis, *Nano Lett.*, 2002, **2**, 301.
12 V. Kumar and Y. Kawazoe, *App. Phys. Lett.*, 2002, **80**, 859.
13 J. Lu and S. Nagase, *Phys. Rev. Lett.*, 2003, **90**, 115506.
14 P. Sen and L. Mitas, *Phys. Rev. B*, 2003, **68**, 155404.
15 V. Kumar, A. K. Singh and Y. Kawazoe, *Nano Lett.*, 2004, **4**, 677.
16 J. Lu and S. Nagase, *Chem. Phys. Lett.*, 2003, **372**, 394.
17 V. Kumar and Y. Kawazoe, *App. Phys. Lett.*, 2003, **83**, 2677.
18 Q. Sun, Q. Wang, T. M. Briere, V. Kumar, Y. Kawazoe and P. Jena, *Phys. Rev. B*, 2002, **65**, 235417.
19 F. Hagelberg, C. Xiao and W. A. Lester, *Phys. Rev. B*, 2003, **67**, 35426.
20 S. Neukermans, E. Janssens, Z. F. Chen, R. E. Silverans, P. V. Schleyer and P. Lievens, *Phys. Rev. Lett.*, 2004, **92**, 163401.
21 H. Hiura, T. Miyazaki and T. Kanayama, *Phys. Rev. Lett.*, 2001, **86**, 1733.

22 X. Zhang, G. L. Li, X. P. Xing, X. Zhao, Z. C. Tang and Z. Gao, *Rapid Commun. Mass Spectrom.*, 2001, **15**, 2399.

23 (*a*) K. Wade, *Adv. Inorg. Chem. Radiochem*, 1976, **18**, 1; (*b*) J. D. Corbett, *Modern Perspective in Inorganic Crystal Chemistry*; NATO ASI, E. Parté, Ed., Kluwer Acad. Publ., Dordrecht, Holland, 1992; p 27.

24 C. Schrodt, F. Weigend and R. Ahlrichs, *Z. Anorg. Allg. Chem.*, 2002, **628**, 2478.

25 S. C. Sevov and J. D. Corbett, *J. Am. Chem. Soc.*, 1993, **115**, 9089.

26 T. F. Fassler, H. J. Muhr and M. Hunziker, *Eur. J. Inorg. Chem.*, 1998, 1433.

27 E. N. Esenturk, J. Fettinger and B. Eichhorn, results to be published.